1

2

3

4

Astrocytes release prostaglandin E2 to modify respiratory network activity

6

7

8 **David Forsberg, Thomas Ringstedt, and Eric Herlenius**

9
10
11
12
13 Department of Women's and Children's Health, Karolinska Institutet, and Karolinska
14 University Hospital, Stockholm, Sweden
15
16
17
18
19
20
21
22
23 Corresponding author
24 Eric Herlenius, MD, PhD
25 Department of Women's and Children's Health
26 Karolinska Institutet and University Hospital
27 171 76 Sweden
28 Tel: 00 46 (0) 5177 5004
29 Email: Eric.herlenius@ki.se

30 **Abstract**

31 Prostaglandin E2 (PGE2) released during hypercapnic challenge increases Ca^{2+} oscillation
32 frequency in the chemosensitive parafacial respiratory group (pFRG/RTN). Here, we
33 demonstrate that pFRG/RTN astrocytes are the PGE2 source. Two distinct astrocyte subtypes
34 were found using transgenic mice expressing GFP and MrgA1 receptors in astrocytes.
35 Although most astrocytes appeared dormant during time-lapse calcium imaging, a subgroup
36 displayed persistent, rhythmic oscillating calcium activity. These active astrocytes formed a
37 subnetwork within the respiratory network distinct from the neuronal network. Activation of
38 exogenous MrgA1 receptors expressed in astrocytes tripled their calcium oscillation
39 frequency activity in both the preBötzinger complex and pFRG/RTN. However, neurons in
40 the preBötC were unaffected, whereas neuronal calcium oscillatory frequency in pFRG/RTN
41 doubled. Notably, astrocyte activation in pFRG/RTN triggered local PGE2 release and
42 blunted the hypercapnic response. Thus, astrocytes play an active role in respiratory rhythm
43 modulation, modifying respiratory-related behaviorthrough PGE2 release in the pFRG/RTN.

Introduction

In the last decade, it has become evident that astrocytes are involved in respiratory behavior; electrically active astrocytes are present in the brainstem respiratory center the preBötzinger Complex (preBötC) (Grass, Pawlowski et al. 2004) and exhibit rhythmic calcium (Ca^{2+}) oscillations associated with the respiratory-related neuronal rhythm (Schnell, Fresemann et al. 2011, Okada, Sasaki et al. 2012). Further, brainstem astrocytes respond to changes in blood gas levels (Angelova, Kasymov et al. 2015), especially in the chemosensitive region the parafacial respiratory group/retrotrapezoid nucleus (pFRG/RTN) (Huckstepp, Bihi et al. 2010). During the hypercapnic response, carbon dioxide (CO_2) causes a vesicle-dependent release of ATP from astrocytes (Fukuda, Honda et al. 1978, Erlichman, Leiter et al. 2010, Gourine, Kasymov et al. 2010, Huckstepp, Bihi et al. 2010, Turovsky, Karagiannis et al. 2015, Turovsky, Theparambil et al. 2016). ATP may also be released in a vesicle independent manner through CO_2-sensitive gap junctions (Huckstepp, Bihi et al. 2010, Huckstepp, Eason et al. 2010, Meigh, Greenhalgh et al. 2013). ATP then increases inspiratory frequency through actions on P2 receptors located in neurons in both the pFRG/RTN and the preBötC (Lorier, Huxtable et al. 2007, Gourine, Kasymov et al. 2010). Acting via EP3 receptors, prostaglandin E2 (PGE2) also alters respiratory network activity by inhibiting signaling frequency in the preBötC while increasing it in the pFRG/RTN (Forsberg, Horn et al. 2016). Additionally, the response to hypercapnic and hypoxic challenges are blunted by PGE2 (Hofstetter, Saha et al. 2007, Siljehav, Olsson Hofstetter et al. 2012, Siljehav, Hofstetter et al. 2015). Because PGE2 is released through gap junctions during hypercapnia, and since some astrocytes in the pFRG/RTN express the primary enzyme involved in PGE2 synthesis (i.e., mPGEs-1) (Forsberg, Horn et al. 2016), we hypothesized that hypercapnia induces astrocytes to release PGE2 in addition to ATP. Thus, astrocytes may also modulate respiratory-related network rhythms via the downstream actions of PGE2.
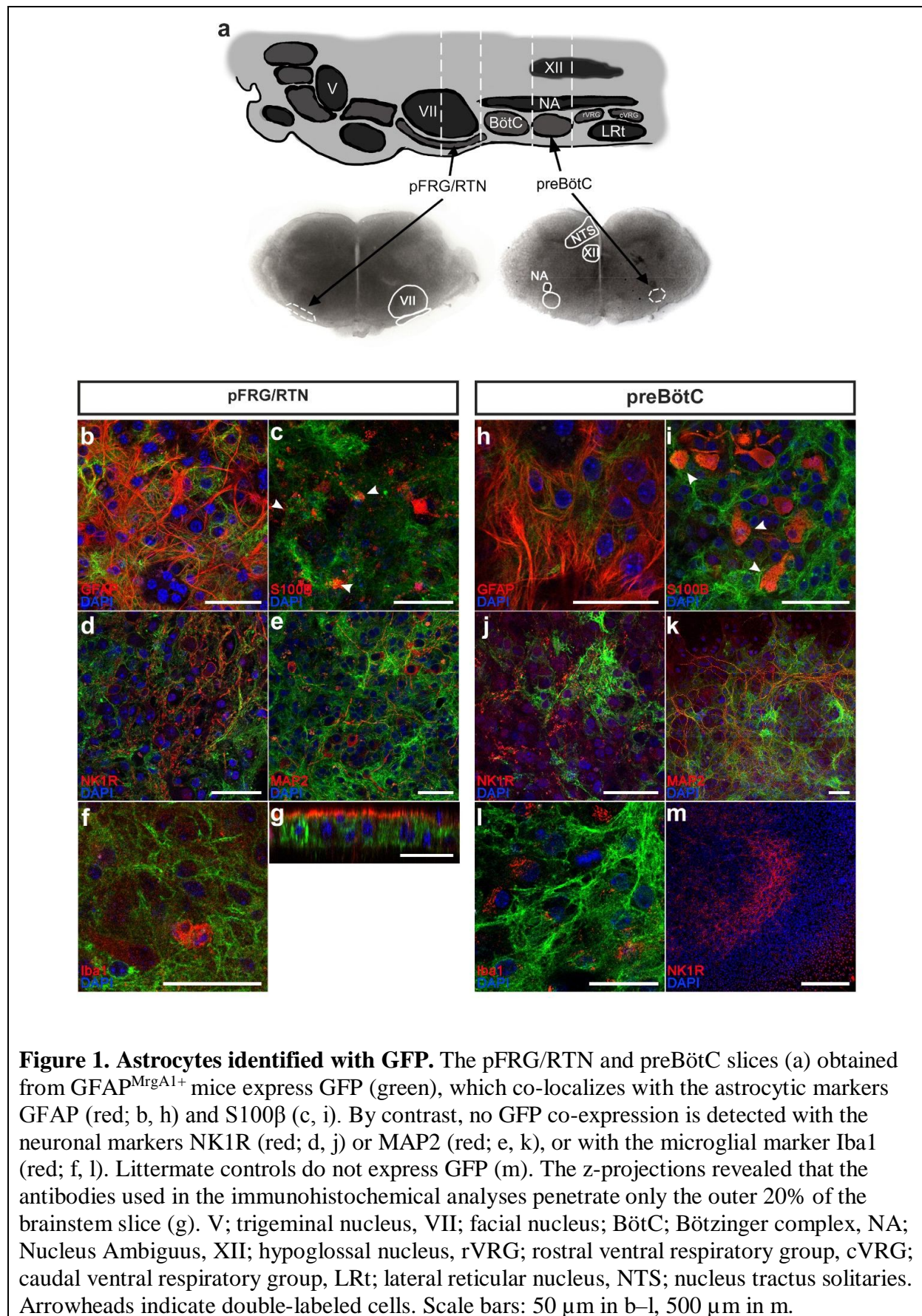
69   To investigate the role of astrocytes in respiratory rhythm-generating networks and

70   determine whether astrocytes release PGE2, we utilized organotypic brainstem slice cultures

71   (Forsberg, Horn et al. 2016, Phillips, Herly et al. 2016) of B6.Cg-Tg(hGFAP-tTA:: tetO-

72   MrgA1)1$^{Kdmc/Mmmh}$ mice (GFAP^{MrgA1+}) in which green fluorescent protein (GFP) and the

73   MrgA1 receptor (MrgA1R) were expressed under control of the promoter for glial fibrillary

74   acidic protein (GFAP), a generally used marker for astrocytes (Brenner, Kisseberth et al.

75   1994). The MrgA1R is an endogenous G_q-coupled receptor that is normally not expressed in

76   the brain. Rather, MrgA1R is expressed exclusively in the dorsal root ganglion nociceptive

77   sensory terminals of the spinal cord (Fiacco, Agulhon et al. 2007) and is activated by RF

78   peptides (Dong, Han et al. 2001). Consequently, we could selectively activate brainstem

79   astrocytes using synthetic Phe-Leu-Arg-Phe-amide (FLRF) (Young, Platel et al. 2010, Cao, Li

80   et al. 2013).

81

82   **Results and Discussion**

83   Expression of GFP in the pFRG/RTN and preBötC of the GFAP^{MrgA1+} mice was evident

84   (**Figure 1**), and GFP was co-localized with GFAP immunolabeling (**Figure 1b and h**, n = 11

85   slices; see **Table 1** for the number of times each experiment was conducted). Although

86   subgroups of GFAP-expressing cells have been previously defined using fluorescence

87   intensity (Grass, Pawlowski et al. 2004), we were unable to detect measurable differences in

88   the GFP fluorescence among our samples. The astrocyte and oligodendrocyte marker S100β

89   was expressed by 12% ± 3% of the GFP-positive cells (n = 13 slices). Conversely, 92% ± 4%

90   of the S100β-positive cells also expressed GFP (**Figure 1c and i,** n = 13 slices). The GFP-

91   positive cells followed the neuronal spread but expressed neither the neuronal markers NK1R

92   or MAP2 (**Figure 1d, e and j, k,** n = 21 slices) nor the microglial marker Iba1 (**Figure 1f and**

93   **l**, n = 11 slices). No GFP expression was detected in littermate controls (WT; **Figure 1m**, n =

4

94   12 slices). These findings confirm that the GFAP-driven expression of GFP (and thus

95   MrgA1R) is astrocyte specific, as expected (Brenner, Kisseberth et al. 1994, Fiacco, Agulhon

96   et al. 2007, Cao, Li et al. 2013). However, the antibodies in our immunohistochemistry

97   experiments penetrated only approximately 20% of the brainstem slice thickness (**Figure 1g**),

98   which must be considered when the organotypic slice culture method is used.
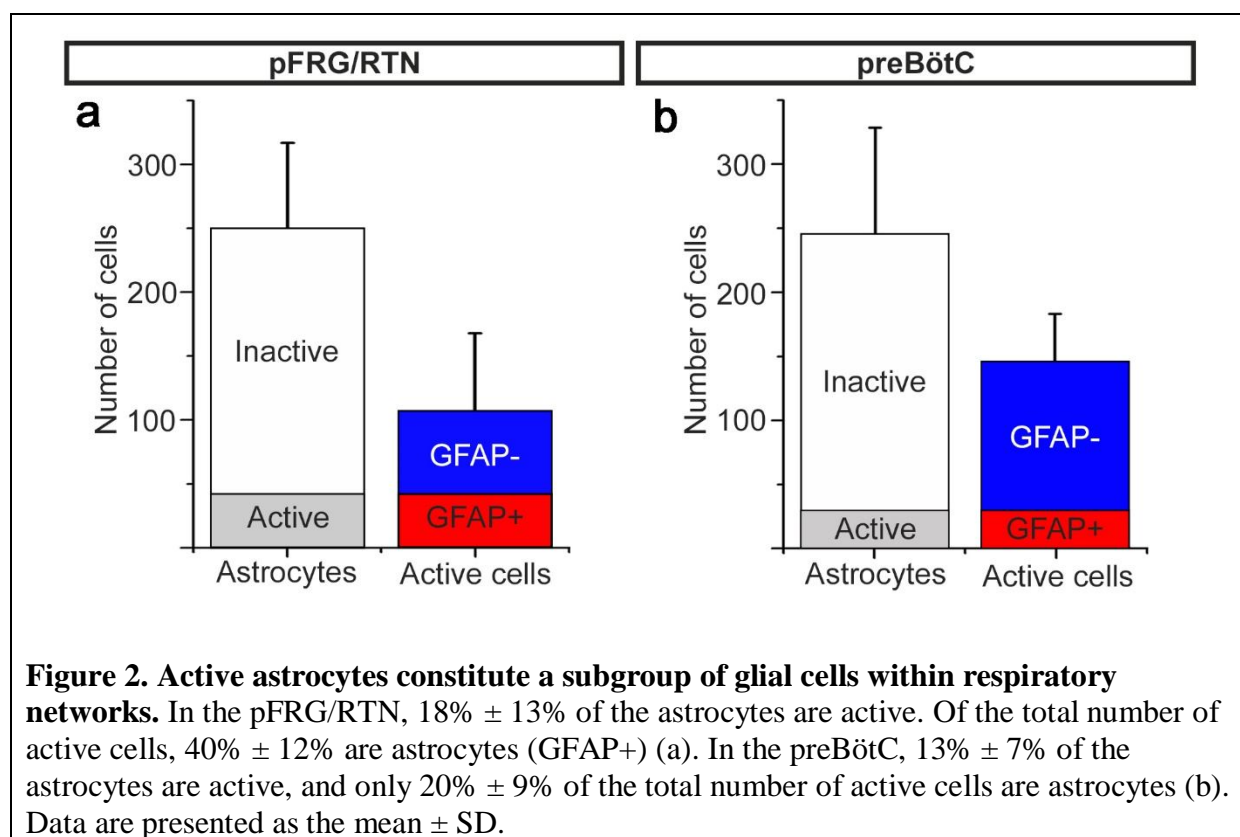
99

Figure 1. Astrocytes identified with GFP. The pFRG/RTN and preBötC slices (a) obtained from GFAP^{MrgA1+} mice express GFP (green), which co-localizes with the astrocytic markers GFAP (red; b, h) and S100β (c, i). By contrast, no GFP co-expression is detected with the neuronal markers NK1R (red; d, j) or MAP2 (red; e, k), or with the microglial marker Iba1 (red; f, l). Littermate controls do not express GFP (m). The z-projections revealed that the antibodies used in the immunohistochemical analyses penetrate only the outer 20% of the brainstem slice (g). V; trigeminal nucleus, VII; facial nucleus; BötC; Bötzinger complex, NA; Nucleus Ambiguus, XII; hypoglossal nucleus, rVRG; rostral ventral respiratory group, cVRG; caudal ventral respiratory group, LRt; lateral reticular nucleus, NTS; nucleus tractus solitaries. Arrowheads indicate double-labeled cells. Scale bars: 50 µm in b–l, 500 µm in m.

112   The Ca^{2+} time-lapse imaging of brainstem slices derived from both GFAP^{MrgA1+} and WT

113   control mice displayed similar average Ca^{2+} signaling frequency and network structure. Thus,

114   the induced expression of GFP and MrgA1R did not affect respiratory network activity or

115   function. Taken together with the results of the immunohistochemical expression analyses,

116   this demonstrates that the MrgA1 mouse line has astrocyte-specific expression of the inserted

117   genes, which display no physiological effects, making this mouse line useful for investigating

118   the role of astrocytes in respiratory networks.

119   We examined the Ca^{2+}-signaling activity of cells in the pFRG/RTN and in the preBötC

120   and identified two subgroups among the GFP-expressing astrocytes: cells with a rhythmic

121   Ca^{2+}-signaling pattern, and cells that appeared inactive, that is, the Fura-2 fluorescence

122   intensity in these cells was stable over time. A similar subgrouping of astrocytes, with

123   approximately 10% exhibiting calcium transients preceding inspiratory-related neuronal

124   signals, has been suggested previously on the basis of both electrophysiological and Ca^{2+}

125   imaging methods (Grass, Pawlowski et al. 2004, Schnell, Fresemann et al. 2011, Oku,

126   Fresemann et al. 2016). The present study also found that the majority of the astrocytes

127   appeared inactive (**Figure 2a and b**; 82% ± 9% in the pFRG/RTN, n = 19 slices; 87% ± 7%

128   in the preBötC, n = 22 slices). In the preBötC, the proportion of active astrocytes was similar

129   to that detected by Schnell and colleagues (Schnell, Fresemann et al. 2011), but lower than

130   that reported by both Grass and colleagues (Grass, Pawlowski et al. 2004) and Oku and

131   colleagues (Oku, Fresemann et al. 2016). However, our data are presented as the proportion

132   per respiratory network, whereas previous studies evaluated the proportion of the total number

133   of recorded cells, independent of individual networks. To our knowledge, the present study is

134   the first to describe active and inactive astrocytes within the pFRG/RTN. Notably, we

135   observed the following difference between the pFRG/RTN and the preBötC: 40% ± 12% of

136   the active cells in pFRG/RTN were astrocytes, whereas only 20% ± 9% of active cells in the

137   preBötC were astrocytes (**Figure 2a and b**, $p < 0.05$ when comparing the pFRG/RTN and the

138   preBötC, n = 41 slices; see **Table 2** for a list of all statistical tests used for all comparisons in

139   the present study).

140   On the basis of a correlated cell activity analysis (Smedler, Malmersjo et al. 2014,

141   Forsberg, Horn et al. 2016), we determined that the active astrocytes within the pFRG/RTN

142   and within the preBötC formed specific networks. These networks differed from those of non-

143   astrocytes, that is, neurons (**Figure 3a and b;** see **Table 1** for the number of times each

144   experiment was conducted), but displayed similar network structures (**Figure 3c and e**). The

145   astrocytic and neuronal networks connected with each other at multiple nodes, and together

146   they formed the respiratory networks of the pFRG/RTN and of the preBötC. In the

147   pFRG/RTN, astrocytes constituted $37\% \pm 13\%$ of the total network (number of correlating

148   cell pairs), whereas astrocytes made up only $16\% \pm 5\%$ of the preBötC network ($p < 0.05$

149   when comparing the pFRG/RTN and the preBötC; **Figure 3a, d, b and f**). We also observed a

150   significantly larger number of connections between astrocytes and neurons in the pFRG/RTN

151   than in the preBötC ($33\% \pm 12\%$ vs. $24\% \pm 11 \%$ of all correlating cell pairs, $p < 0.05$; **Figure**

152   **3a, b, d and f**). Thus, astrocytes are both independently active and part of the respiratory

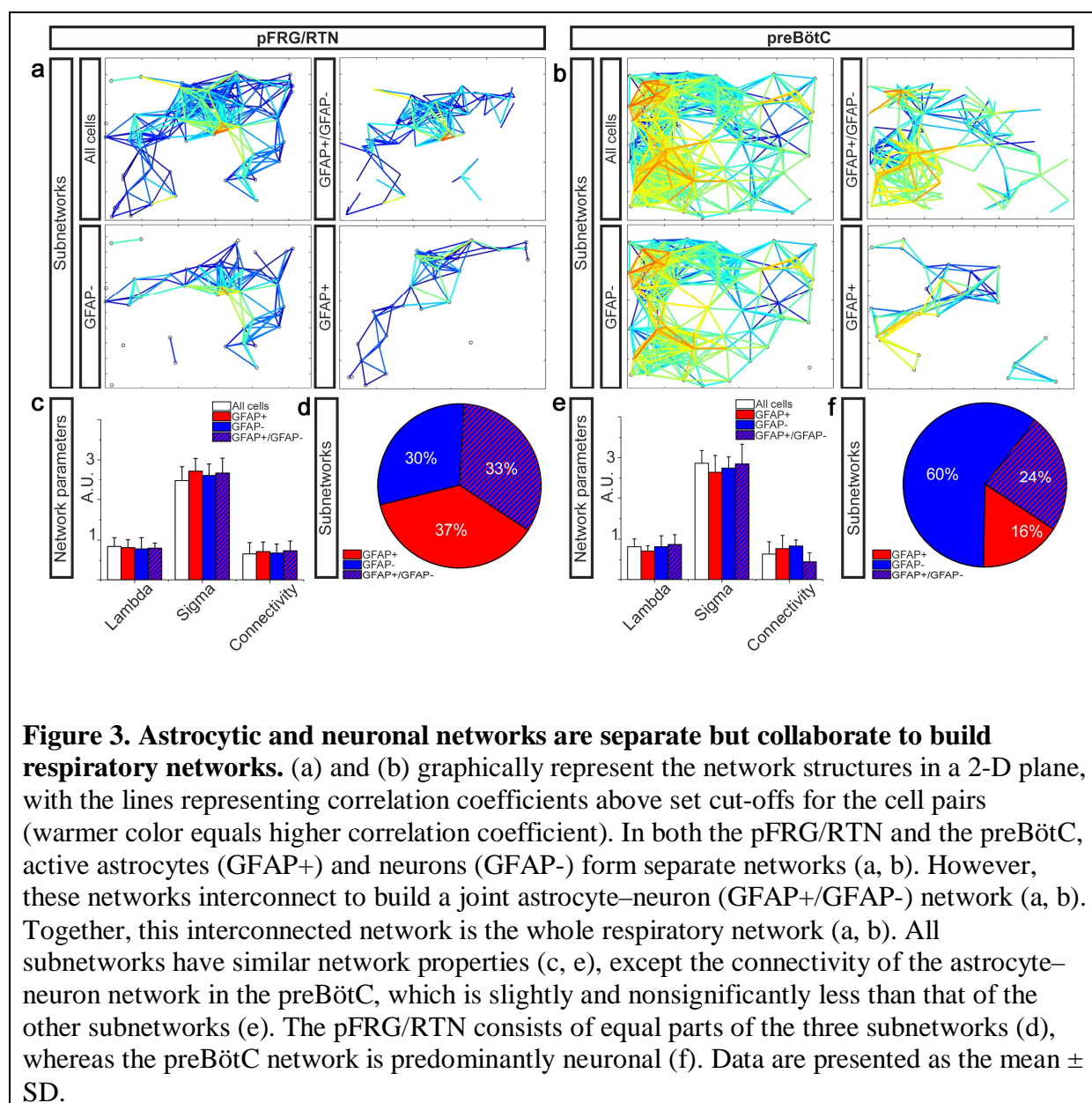153   networks, but appear to have different actions in the two central pattern generators.

154

155

156

157 **Figure 2. Active astrocytes constitute a subgroup of glial cells within respiratory**
158 **networks.** In the pFRG/RTN, 18% ± 13% of the astrocytes are active. Of the total number of
159 active cells, 40% ± 12% are astrocytes (GFAP+) (a). In the preBötC, 13% ± 7% of the
160 astrocytes are active, and only 20% ± 9% of the total number of active cells are astrocytes (b).
161 Data are presented as the mean ± SD.

162

Figure 3. Astrocytic and neuronal networks are separate but collaborate to build respiratory networks. (a) and (b) graphically represent the network structures in a 2-D plane, with the lines representing correlation coefficients above set cut-offs for the cell pairs (warmer color equals higher correlation coefficient). In both the pFRG/RTN and the preBötC, active astrocytes (GFAP+) and neurons (GFAP-) form separate networks (a, b). However, these networks interconnect to build a joint astrocyte–neuron (GFAP+/GFAP-) network (a, b). Together, this interconnected network is the whole respiratory network (a, b). All subnetworks have similar network properties (c, e), except the connectivity of the astrocyte–neuron network in the preBötC, which is slightly and nonsignificantly less than that of the other subnetworks (e). The pFRG/RTN consists of equal parts of the three subnetworks (d), whereas the preBötC network is predominantly neuronal (f). Data are presented as the mean ± SD.

10

177   Under control conditions, astrocytes displayed a low oscillating frequency (19 ± 8 mHz

178   in the preBötC (n = 22 slices) vs. 18 ± 7 mHz in the pFRG (n = 19 slices); difference not

179   statistically significant), similar to that described previously for active astrocytes (Grass,

180   Pawlowski et al. 2004, Schnell, Fresemann et al. 2011, Okada, Sasaki et al. 2012, Oku,

181   Fresemann et al. 2016). The frequency displayed by the astrocytes in each region was lower

182   than that shown by the neurons in the respective regions (preBötC: 90 ± 40 mHz, n = 22

183   slices, $p < 0.05$ compared with astrocytes; pFRG: 106 ± 58 mHz, n = 19 slices, $p < 0.05$

184   compared with astrocytes). We did not register nerve output signals in the present study and

185   can therefore not evaluate whether astrocytic signaling was phase-locked with the respiratory

186   output.

187   Next, we activated the GFAP^{MrgA1+} astrocytes by applying the MrgA1R ligand FLRF,

188   which increased the Ca^{2+}-signaling frequency of astrocytes in both the pFRG/RTN and the

189   preBötC (**Figure 4a and b**). In the pFRG/RTN, astrocyte activation also induced an increase

190   in the signaling frequency of the non-astrocytes (**Figure 4a and b**). This is in contrast to the

191   preBötC, wherein non-astrocytes retained their Ca^{2+}-signaling frequency independent of

192   astrocyte stimulation (**Figure 4a and b**). Inactive astrocytes showed a single Ca^{2+} peak

193   shortly after the application of FLRF, but returned to the inactive state within 10 s (**Figure

194   4a**). The stimulation of astrocytes did not affect the network structures of the astrocytic,

195   neuronal, or complete respiratory networks (**Figure 4c**). Astrocytes in slices derived from WT

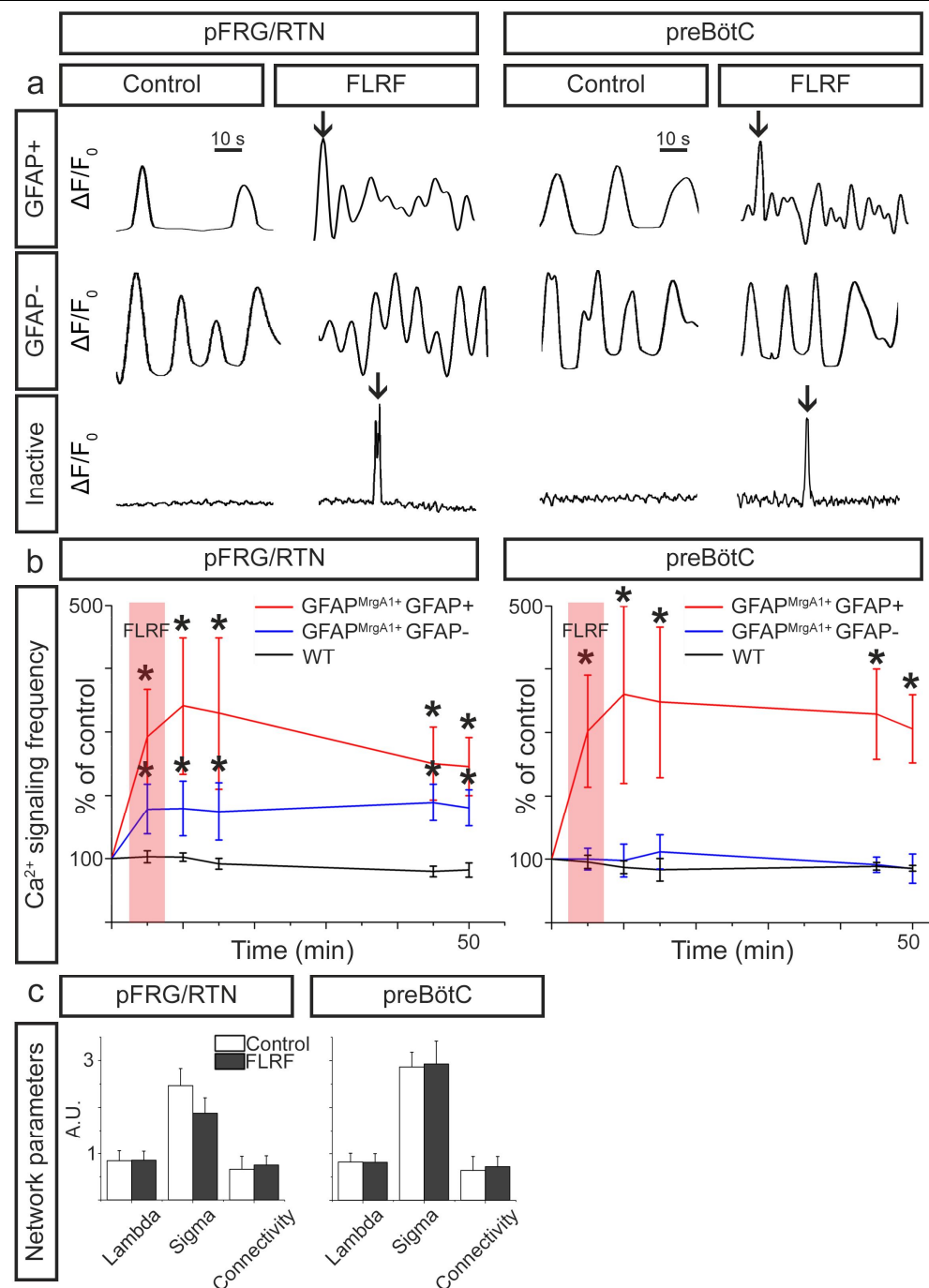196   mice did not react to the application of FLRF (**Figure 4b**).

197

Figure 4. Astrocytes control neurons in the pFRG/RTN. (a) Individual 1 min calcium traces ($\Delta F/F_0$ over time, band pass filtered 0.01–0.15 Hz) during the control period and after the application of the MrgA1R ligand FLRF. Activation of astrocytes through addition of FLRF increases calcium-signaling frequency of astrocytes in both the pFRG/RTN and the preBötC (b, red trace). In the pFRG/RTN, neuronal calcium-signaling frequency increases after astrocyte activation (b, blue trace). This is not observed in the preBötC (b, blue trace). Littermate controls (WT) do not respond to FLRF (b, black trace). Network properties are not affected by addition of FLRF (c). Data are presented as the mean ± SD. *p < 0.05 compared to their respective controls.

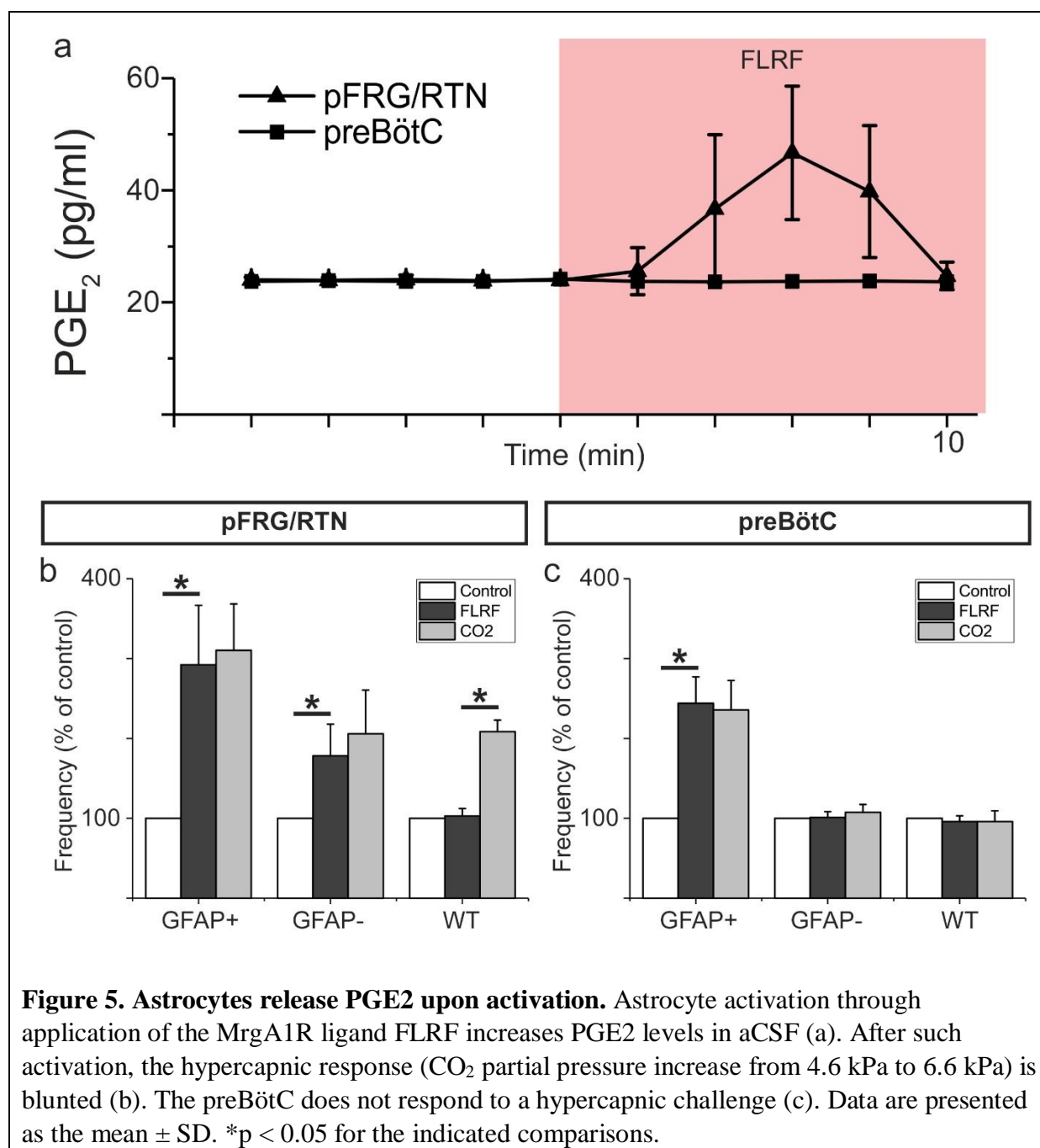208 While these findings suggest that astrocytes do not directly modify neuronal activity in the

209 preBötC, astrocytes may, nonetheless, be important for the maintenance of the respiratory

210 rhythm generation in this complex. For instance, the astrocyte inhibitor methionine

211 sulfoximine depresses breathing in vivo (Young, Dreshaj et al. 2005), and glial inhibitors

212 (fluorocitrate, fluoroacetate, and methionine sulfoximine) reduce respiratory-related activity

213 in the preBötC in vitro (Erlichman, Li et al. 1998, Huxtable, Zwicker et al. 2010). In addition,

214 hypoxia can induce a Ca^{2+} influx in preBötC astrocytes, inducing a release of ATP (Gourine,

215 Llaudet et al. 2005, Angelova, Kasymov et al. 2015). This helps to maintain the inspiratory-

216 related rhythm generation in the preBötC during post-hypoxic depression (Gourine, Llaudet et

217 al. 2005). Although we did not measure an increase in neuronal network burst frequency after

218 astrocyte-specific activation, we did not test responses under hypoxic conditions.

219   Our data suggest that, in contrast to their function in the preBötC, astrocytes in the

220 pFRG/RTN modulate respiratory network activity. This corroborates the results of previous

221 studies that have demonstrated the involvement of astrocytes in chemosensitivity through

222 purinergic signaling (Erlichman, Leiter et al. 2010, Gourine, Kasymov et al. 2010, Huckstepp,

223 Bihi et al. 2010, Gourine and Kasparov 2011, Angelova, Kasymov et al. 2015). In one of our

224 recent articles, we suggested that astrocytes release PGE2 (in addition to ATP) in response to

225 a hypercapnic challenge (Forsberg, Horn et al. 2016). This would in part explain the

226 interaction between chemosensitivity and the inflammatory system observed in several studies

227 (Hofstetter, Saha et al. 2007, Siljehav, Olsson Hofstetter et al. 2012, Siljehav, Shvarev et al.

228 2014, Forsberg, Horn et al. 2016). Moreover, in human neonates, rapid elevation of brainstem

229 PGE2 during infectious events is associated with and may explain the initial presenting

230 symptoms of infection, which are apnea, bradycardia, and desaturation (Siljehav, Hofstetter et

231 al. 2015).

232

13

233   Because a hypercapnic challenge triggers a gap junction mediated release of PGE2

234   (Forsberg, Horn et al. 2016), we hypothesized that astrocyte stimulation would trigger a

235   similar release. Indeed, we found that after FLRF application, the PGE2 levels in the artificial

236   cerebrospinal fluid (aCSF) doubled in the pFRG/RTN (**Figure 5a**, n = 8 slices, p < 0.05). The

237   increase was transient, similar to the PGE2 release that occurs during hypercapnia (Forsberg,

238   Horn et al. 2016). By contrast, the PGE2 levels remained unaffected by FLRF application in

239   the GFAP^{MrgA1+} preBötC slices (n = 3 slices) and both the pFRG/RTN and preBötC regions in

240   the WT slices (n = 2 slices for each region). These results indicated that the pFRG/RTN

241   contains chemosensitive astrocytes that release PGE2 upon hypercapnic challenge. The

242   physiological effect of the released PGE2 is likely multifactorial. We previously demonstrated

243   that PGE2 is involved in the stimulation of the pFRG/RTN (Forsberg, Horn et al. 2016),

244   similar to the effects of ATP (Gourine, Kasymov et al. 2010). Although ATP counteracts the

245   vasodilatory effect of CO_2/H^+ during hypercapnia in the ventral brainstem (Hawkins,

246   Takakura et al. 2017), the role of PGE2 in the microcircuits controlling brainstem blood flow

247   will require further investigation.

248   We also determined that pre-activation of astrocytes blunts the hypercapnic response in

249   the pFRG/RTN (**Figure 5b**, n = 8 slices). This result suggested that existing PGE2, and likely

250   other gliotransmitters, is released after activation, depleting the stores. Extracellular pH is

251   retained during hypercapnia in our system (Forsberg, Horn et al. 2016), but CO_2 can pass over

252   the cell membrane and decrease the intracellular pH. This decreased pH drives bicarbonate

253   and sodium ions into the cell, triggering a Ca^{2+} influx (Turovsky, Theparambil et al. 2016). In

254   parallel, CO_2 can directly modify connexin 26 hemichannels to induce an open state

255   (Huckstepp, Bihi et al. 2010, Meigh, Greenhalgh et al. 2013). Thus, it is possible that the

256   mechanism behind the gliotransmitter release during hypercapnic challenge is different from

257   that of the FLRF-induced activation and Ca^{2+} influx. The design of the present study could

14

258   not discern between PGE2 released from active and inactive astrocytes or determine whether

259   PGE2 directly affected neurons or acted via intermediate astrocytes. In the pFRG/RTN,

260   prostaglandin EP3 receptors have been found on both neurons and astrocytes (Forsberg, Horn

261   et al. 2016). Thus, the different pathways as well as the kinetics associated with the effects of

262   PGE2 will require further investigation. Hypercapnia did not affect the preBötC activity

263   (**Figure 5c**, n = 6 slices), consistent with the results of our previous study (Forsberg, Horn et

264   al. 2016). In summary, these results indicated that the pFRG/RTN contains astrocytes that are

265   able to react to CO_2 and release PGE2 (and possibly other gliotransmitters) to modify the

266   behavior of the neuronal population. This type of astrocytic responsiveness and modifying

267   effect was not detected in the preBötC.

Figure 5. Astrocytes release PGE2 upon activation. Astrocyte activation through application of the MrgA1R ligand FLRF increases PGE2 levels in aCSF (a). After such activation, the hypercapnic response (CO_2 partial pressure increase from 4.6 kPa to 6.6 kPa) is blunted (b). The preBötC does not respond to a hypercapnic challenge (c). Data are presented as the mean $\pm$ SD. *$p < 0.05$ for the indicated comparisons.

275   Taken together, our results led us to conclude that a subgroup of astrocytes with

276   oscillatory Ca^{2+} activity interacted with and was an essential part of the respiratory neural

277   networks. We observed that almost half of the cells in the pFRG/RTN network were

278   astrocytes and that these astrocytes could entrain the neuronal rhythm, suggesting that

279   pFRG/RTN astrocytes are a source of gliotransmitters that modify respiratory activity.

280   Moreover, a transient release of PGE2 induced by a Ca^{2+} influx in the astrocytes of the

281   pFRG/RTN substantially reduced the subsequent hypercapnic response, suggesting a central

282   role of PGE2 as a gliotransmitter in chemosensitivity. Thus, subgroups of astrocytes

283   participate in the respiratory rhythm of both the preBötC and the pFRG/RTN, and modify

284   respiratory network behavior in the pFRG/RTN. Therefore, we suggest that astrocytes

285   constitute an important link between the respiratory and inflammatory systems, and stand out

286   as a potential target for the treatment of central respiratory dysfunction.

287

Materials and Methods

Subjects

Mice expressing green fluorescent protein (GFP) under the GFAP promoter were used. Frozen sperm from the GFAP-tTA (Lin, Kemper et al. 2004, Pascual, Casper et al. 2005) and tetO-Mrgpra1 (Fiacco, Agulhon et al. 2007) mouse strains were purchased from the Mutant Mouse Resource and Research Center (MMRRC) supported by the National Institutes of Health. The strains were re-derived by the Karolinska Center for Transgene Technologies, and the offspring were crossed as previously described (Fiacco, Agulhon et al. 2007). The double transgenic B6.Cg-Tg(hGFAP-tTA::tetO-MrgA1)[1Kdmc/Mmmh] mice were identified by polymerase chain reaction analyses according to instructions provided by the MMRRC.

All mice were reared by their mothers under standardized conditions with a 12 h light–dark cycle. The mice were allowed food and water ad libitum. The studies were performed in accordance with European Community Guidelines and approved by the regional ethics committee. The animals were reared and kept in the Department of Comparative Medicine at the Karolinska Institute in Stockholm, Sweden.

Brainstem organotypic culture

Mouse pups were used at postnatal day 3 for the establishment of brainstem organotypic slice cultures (Herlenius, Thonabulsombat et al. 2012, Forsberg, Horn et al. 2016). Transverse slices (300 µm thick) were maintained in culture for 7 to 14 days. Slices were selected by using online anatomical references (Ruangkittisakul, Schwarzacher et al. 2006, Ruangkittisakul, Panaitescu et al. 2011, Ruangkittisakul, Kottick et al. 2014).

Immunohistochemistry

18

312   The immunohistochemistry procedure was the same as that described previously (Forsberg,

313   Horn et al. 2016).). The primary antibodies used were mouse anti-microtubule associated

314   protein 2 (MAP2; Invitrogen, cat. no. P11137), rabbit anti-neurokinin 1 receptor (NK1R;

315   Sigma-Aldrich, St. Louis, MO, USA, cat no. S8305), mouse anti-GFAP (Chemicon,

316   Temecula, CA, USA, cat no. MAB360), rabbit anti-S100β (Millipore; cat. no. 04-1054),

317   rabbit anti-Iba1 (Wako, Japan; cat. no. 019-19741) and goat anti-GFP (Abcam, Cambridge,

318   United Kingdom; cat. no. Ab6673). The secondary antibodies used were Alexa Fluor Plus 555

319   goat anti-mouse IgG (Thermo Fisher Scientific, Waltham, MA, USA; cat. no. A32737), Alexa

320   Fluor Plus 555 goat anti-rabbit IgG (Thermo Fisher Scientific, Waltham, MA, USA; cat. no.

321   A32732), Alexa Fluor 555 donkey anti-rabbit (Thermo Fisher Scientific, Waltham, MA,

322   USA; cat. no. A31572) and Alexa Fluor 488 donkey anti-goat (Thermo Fisher Scientific,

323   Waltham, MA, USA; cat. no. A11055). Negative control tissue incubated in the absence of

324   primary antibodies showed no staining.

325

326   **Ca^{2+} time-lapse imaging**

327   For Ca^{2+} imaging, Fura-2 AM (Thermo Fisher Scientific, Waltham, MA, USA; cat. no.

328   F1201) dissolved in DMSO (Sigma-Aldrich, St. Louis, MO, USA, cat. no .D2650) was used

329   at 166 µM in aCSF (containing in mM: 150.1 Na^+, 3 K^+, 2 Ca^{2+}, 2 Mg^{2+}, 135 Cl^-, 1.1 $H_2PO_4^-$,

330   25 HCO_3^- and 10 glucose) together with 0.02% pluronic acid (Thermo Fisher Scientific,

331   Waltham, MA, USA cat. no. P3000MP). To localize the preBötC or the pFRG/RTN,

332   tetramethylrhodamine-conjugated substance P (TMR-SP; Biomol, Oakdale, NY, USA) was

333   used at a final concentration of 3 µM in aCSF. The TMR-SP solution was placed on top on

334   the brainstem slice and incubated for 10 min at 37°C in an atmosphere of 5% CO_2. Brainstem

335   slices were incubated in the TMR-SP solution for 10 min at 37°C in an atmosphere of 5%

336   CO_2. The TMR-SP solution was then replaced with 1.5 ml of 166 µM Fura-2 solution. The

337   Fura-2 solution was incubated for 30 min at room temperature. Before imaging, the slice was

338   washed with aCSF for 10 min (32°C, 5% CO_2).

339   During time-lapse imaging, slices were kept in an open chamber perfused with aCSF (1.5

340   mL/min), as described previously (Forsberg, Horn et al. 2016). The exposure time was set to

341   100 ms, with an imaging interval of 0.5 s. During imaging, FLRF (10 µM in 0.1% DMSO in

342   aCSF; Innovagen, Lund, Sweden) was added continuously for 5 min after a control period. A

343   subset of slices was exposed to isohydric hypercapnia, with the aCSF adjusted with a high-

344   bicarbonate buffer concentration (in mM: 150.1 Na^+, 3 K^+, 2 Ca^{2+}, 2 Mg^{2+}, 111 Cl^-, 1.1

345    $H_2PO_4^-$, 50 HCO_3^-, and 10 glucose) saturated with 8% CO_2. This generated a hypercapnic

346   carbon dioxide partial pressure (pCO_2) of 6.6 kPa at pH 7.5.

347

348   **PGE_2 enzyme-linked immunosorbent assay (ELISA)**

349   The release of PGE_2 in aCSF during FLRF exposure was assessed by ELISA. The aCSF

350   samples were collected through the perfusion system each minute and stored at −80°C. The

351   prostaglandin E_2 EIA monoclonal kit (Cayman Chemicals, Ann Arbor, MI, USA, cat. no.

352   514010) was used according to our previously published procedure (Forsberg, Horn et al.

353   2016).

354

355   **Data analysis**

356   Data were analyzed as previously described (Forsberg, Horn et al. 2016).

357

358   **Statistics**

359   Statistical analysis of paired comparisons was performed by Student's *t*-test. Full factorial

360   analysis of variance (ANOVA) was performed when more than one independent variable was

361   compared or for multiple comparisons. Both tests were two-sided. The compared data were of

362   equal variance and normally distributed. All calculations for the statistical tests were

363   conducted with JMP software (version 11.1., SAS Institute Inc., Cary, NC, USA). In all cases,

364   values of p <0.05 were considered statistically significant. Data are presented as means ± SD.

365   All data sets were compared less than 20 times; thus no statistical corrections were applied.

366   Because these experiments were conducted to provide new descriptive data, no explicit power

367   analysis was performed. Instead, sample sizes similar to previous publications using similar

368   methods were used.

369

376

377   **Competing interests**

378   EH: employed at the Karolinska Institutet and the Karolinska University Hospital and is a

379   coinventor of a patent application regarding biomarkers and their relation to breathing

380   disorders, WO2009063226. The other authors declare that no competing interests exist.

Table 1. Number of experiments conducted

Figure	Panel	Number of experiments
1	b	5
	c	7
	d	6
	e	6
	f	6
	g	5
	h	6
	i	6
	j	5
	k	5
	l	5
	m	6
3	a	19
	b	22

Table 2. Statistical analyses and results

Figure	Test used	Exact p-value	Degrees of freedom & F/t/z/R value
2	Student's t-test	0.0261	DF = 40
3c	Full factorial ANOVA	0.821 0.688 0.716	F=0.071 F=0.043 F=0.052 DFE=18
3e	Full factorial ANOVA	0.416 0.237 0.0946	F=0.064 F=0.065 F=0.038 DFE=21
4b	Student's t-test	0.0213 0.0278 0.0342 0.0413 0.0427	DF=10, 10, 10, 7, 7
		0.0147 0.0129 0.0385 0.0311 0.0406	DF=11, 11, 11, 9, 9
4c	Full factorial ANOVA	0.416 0.759	F=0.029, DFE=6 F=0.063, DFE=7
5a	Student's t-test	0.0729 0.0271 0.0014 0.0298 0.194	DF=7
5b	Student's t-test	0.017, 0.44 0.014, 0.71 0.29, 0.024	DF=8
5c	Student's t-test	0.018, 0.41 0.74, 0.85 0.66, 0.70	DF=7

23

References

Angelova PR, Kasymov V, Christie I, Sheikhbahaei S, Turovsky E, Marina N, Korsak A, Zwicker J, Teschemacher AG, Ackland GL, Funk GD, Kasparov S, Abramov AY and Gourine AV. 2015. Functional Oxygen Sensitivity of Astrocytes. *J Neurosci* **35**:10460-10473. 10.1523/JNEUROSCI.0045-15.2015.

Brenner M, Kisseberth WC, Su Y, Besnard F and Messing A. 1994. GFAP promoter directs astrocyte-specific expression in transgenic mice. *J Neurosci* **14**:1030-1037.

Cao X, Li LP, Wang Q, Wu Q, Hu HH, Zhang M, Fang YY, Zhang J, Li SJ, Xiong WC, Yan HC, Gao YB, Liu JH, Li XW, Sun LR, Zeng YN, Zhu XH and Gao TM. 2013. Astrocyte-derived ATP modulates depressive-like behaviors. *Nat Med* **19**:773-777. 10.1038/nm.3162.

Dong X, Han S, Zylka MJ, Simon MI and Anderson DJ. 2001. A diverse family of GPCRs expressed in specific subsets of nociceptive sensory neurons. *Cell* **106**:619-632.

Erlichman JS, Leiter JC and Gourine AV. 2010. ATP, glia and central respiratory control. *Respir Physiol Neurobiol* **173**:305-311. S1569-9048(10)00227-2 [pii]

10.1016/j.resp.2010.06.009.

Erlichman JS, Li A and Nattie EE. 1998. Ventilatory effects of glial dysfunction in a rat brain stem chemoreceptor region. *J Appl Physiol (1985)* **85**:1599-1604.

Fiacco TA, Agulhon C, Taves SR, Petravicz J, Casper KB, Dong X, Chen J and McCarthy KD. 2007. Selective stimulation of astrocyte calcium in situ does not affect neuronal excitatory synaptic activity. *Neuron* **54**:611-626. S0896-6273(07)00336-4 [pii]

10.1016/j.neuron.2007.04.032.

Forsberg D, Horn Z, Tserga E, Smedler E, Silberberg G, Shvarev Y, Kaila K, Uhlen P and Herlenius E. 2016. CO2-evoked release of PGE2 modulates sighs and inspiration as demonstrated in brainstem organotypic culture. *Elife* **5:e14170**. 10.7554/eLife.14170.

Fukuda Y, Honda Y, Schlafke ME and Loeschcke HH. 1978. Effect of H+ on the membrane potential of silent cells in the ventral and dorsal surface layers of the rat medulla in vitro. *Pflugers Arch* **376**:229-235.

Gourine AV and Kasparov S. 2011. Astrocytes as brain interoceptors. *Exp Physiol* **96**:411-416. 10.1113/expphysiol.2010.053165.

Gourine AV, Kasymov V, Marina N, Tang F, Figueiredo MF, Lane S, Teschemacher AG, Spyer KM, Deisseroth K and Kasparov S. 2010. Astrocytes control breathing through pH-dependent release of ATP. *Science* **329**:571-575. science.1190721 [pii]

10.1126/science.1190721.

Gourine AV, Llaudet E, Dale N and Spyer KM. 2005. Release of ATP in the ventral medulla during hypoxia in rats: role in hypoxic ventilatory response. *J Neurosci* **25**:1211-1218. 10.1523/JNEUROSCI.3763-04.2005.

Grass D, Pawlowski PG, Hirrlinger J, Papadopoulos N, Richter DW, Kirchhoff F and Hulsmann S. 2004. Diversity of Functional Astroglial Properties in the Respiratory Network. *J. Neurosci.* **24**:1358-1365.

Hawkins VE, Takakura AC, Trinh A, Malheiros-Lima MR, Cleary CM, Wenker IC, Dubreuil T, Rodriguez EM, Nelson MT, Moreira TS and Mulkey DK. 2017. Purinergic regulation of vascular tone in the retrotrapezoid nucleus is specialized to support the drive to breathe. *Elife* **6**. 10.7554/eLife.25232.

Herlenius E, Thonabulsombat C, Forsberg D, Jaderstad J, Jaderstad LM, Bjork L and Olivius P. 2012. Functional stem cell integration assessed by organotypic slice cultures. *Curr Protoc Stem Cell Biol* **Chapter 2**:Unit 2D 13. 10.1002/9780470151808.sc02d13s23.

Hofstetter AO, Saha S, Siljehav V, Jakobsson PJ and Herlenius E. 2007. The induced prostaglandin E2 pathway is a key regulator of the respiratory response to infection and hypoxia in neonates. *Proc Natl Acad Sci U S A* **104**:9894-9899. 10.1073/pnas.0611468104.

Huckstepp RT, Bihi R, Eason R, Spyer KM, Dicke N, Willecke K, Marina N, Gourine AV and Dale N. 2010. Connexin hemichannel-mediated CO2-dependent release of ATP in the medulla oblongata contributes to central respiratory chemosensitivity. *J Physiol* **588**:3901-3920. 10.1113/jphysiol.2010.192088.

Huckstepp RT, Eason R, Sachdev A and Dale N. 2010. CO2-dependent opening of connexin 26 and related beta connexins. *J Physiol* **588**:3921-3931. 10.1113/jphysiol.2010.192096.

Huxtable AG, Zwicker JD, Alvares TS, Ruangkittisakul A, Fang X, Hahn LB, Posse de Chaves E, Baker GB, Ballanyi K and Funk GD. 2010. Glia contribute to the purinergic modulation of inspiratory rhythm-generating networks. *J Neurosci* **30**:3947-3958. 30/11/3947 [pii]

10.1523/JNEUROSCI.6027-09.2010.

Lin W, Kemper A, McCarthy KD, Pytel P, Wang JP, Campbell IL, Utset MF and Popko B. 2004. Interferon-gamma induced medulloblastoma in the developing cerebellum. *J Neurosci* **24**:10074-10083. 10.1523/JNEUROSCI.2604-04.2004.

Lorier AR, Huxtable AG, Robinson DM, Lipski J, Housley GD and Funk GD. 2007. P2Y1 Receptor Modulation of the Pre-Botzinger Complex Inspiratory Rhythm Generating Network In Vitro. *Journal of Neuroscience* **27**:993-1005. 10.1523/jneurosci.3948-06.2007.

Meigh L, Greenhalgh SA, Rodgers TL, Cann MJ, Roper DI and Dale N. 2013. CO(2)directly modulates connexin 26 by formation of carbamate bridges between subunits. *Elife* **2**:e01213. 10.7554/eLife.01213.

Okada Y, Sasaki T, Oku Y, Takahashi N, Seki M, Ujita S, Tanaka KF, Matsuki N and Ikegaya Y. 2012. Preinspiratory calcium rise in putative pre-Botzinger complex astrocytes. *J Physiol* **590**:4933-4944. 10.1113/jphysiol.2012.231464.

Oku Y, Fresemann J, Miwakeichi F and Hulsmann S. 2016. Respiratory calcium fluctuations in low-frequency oscillating astrocytes in the pre-Botzinger complex. *Respir Physiol Neurobiol* **226**:11-17. 10.1016/j.resp.2015.02.002.

Pascual O, Casper KB, Kubera C, Zhang J, Revilla-Sanchez R, Sul JY, Takano H, Moss SJ, McCarthy K and Haydon PG. 2005. Astrocytic purinergic signaling coordinates synaptic networks. *Science* **310**:113-116. 10.1126/science.1116916.

Phillips WS, Herly M, Del Negro CA and Rekling JC. 2016. Organotypic slice cultures containing the preBotzinger complex generate respiratory-like rhythms. *J Neurophysiol* **115**:1063-1070. 10.1152/jn.00904.2015.

Ruangkittisakul A, Kottick A, Picardo MC, Ballanyi K and Del Negro CA. 2014. Identification of the pre-Botzinger complex inspiratory center in calibrated "sandwich" slices from newborn mice with fluorescent Dbx1 interneurons. *Physiol Rep* **2**. 10.14814/phy2.12111.

Ruangkittisakul A, Panaitescu B and Ballanyi K. 2011. K(+) and Ca(2)(+) dependence of inspiratory-related rhythm in novel "calibrated" mouse brainstem slices. *Respir Physiol Neurobiol* **175**:37-48. 10.1016/j.resp.2010.09.004.

Ruangkittisakul A, Schwarzacher SW, Secchia L, Poon BY, Ma Y, Funk GD and Ballanyi K. 2006. High sensitivity to neuromodulator-activated signaling pathways at physiological [K+] of confocally imaged respiratory center neurons in on-line-calibrated newborn rat brainstem slices. *J Neurosci* **26**:11870-11880. 26/46/11870 [pii]

10.1523/JNEUROSCI.3357-06.2006.

Schnell C, Fresemann J and Hulsmann S. 2011. Determinants of functional coupling between astrocytes and respiratory neurons in the pre-Botzinger complex. *PLoS One* **6**:e26309. 10.1371/journal.pone.0026309.

Siljehav V, Hofstetter AM, Leifsdottir K and Herlenius E. 2015. Prostaglandin E2 Mediates Cardiorespiratory Disturbances during Infection in Neonates. *J Pediatr* **167**:1207-1213 e1203. 10.1016/j.jpeds.2015.08.053.

Siljehav V, Olsson Hofstetter A, Jakobsson PJ and Herlenius E. 2012. mPGES-1 and prostaglandin E2: vital role in inflammation, hypoxic response, and survival. *Pediatr Res* **72**:460-467. 10.1038/pr.2012.119.

Siljehav V, Shvarev Y and Herlenius E. 2014. Il-1beta and prostaglandin E2 attenuate the hypercapnic as well as the hypoxic respiratory response via prostaglandin E receptor type 3 in neonatal mice. *J Appl Physiol (1985)* **117**:1027-1036. 10.1152/japplphysiol.00542.2014.

Smedler E, Malmersjo S and Uhlen P. 2014. Network analysis of time-lapse microscopy recordings. *Front Neural Circuits* **8**:111. 10.3389/fncir.2014.00111.

Turovsky E, Karagiannis A, Abdala AP and Gourine AV. 2015. Impaired CO2 sensitivity of astrocytes in a mouse model of Rett syndrome. *J Physiol* **593**:3159-3168. 10.1113/JP270369.

Turovsky E, Theparambil SM, Kasymov V, Deitmer JW, Del Arroyo AG, Ackland GL, Corneveaux JJ, Allen AN, Huentelman MJ, Kasparov S, Marina N and Gourine AV. 2016. Mechanisms of CO2/H+ Sensitivity of Astrocytes. *J Neurosci* **36**:10750-10758. 10.1523/JNEUROSCI.1281-16.2016.

Young JK, Dreshaj IA, Wilson CG, Martin RJ, Zaidi SI and Haxhiu MA. 2005. An astrocyte toxin influences the pattern of breathing and the ventilatory response to hypercapnia in neonatal rats. *Respir Physiol Neurobiol* **147**:19-30. 10.1016/j.resp.2005.01.009.

Young SZ, Platel JC, Nielsen JV, Jensen NA and Bordey A. 2010. GABA(A) Increases Calcium in Subventricular Zone Astrocyte-Like Cells Through L- and T-Type Voltage-Gated Calcium Channels. *Front Cell Neurosci* **4**:8. 10.3389/fncel.2010.00008.